JOURNAL OF PETROLOGY

Journal of Petrology, 2019, Vol. 60, No. 3, 649–660
doi: 10.1093/petrology/egy118
Advance Access Publication Date: 31 December 2018
Comment and Reply

OXFORD

Comment on: 'Petrography of the Snap Lake Kimberlite Dyke (Northwest Territories, Canada) and its Interaction with Country Rock Granitoids' by Fulop *et al.* (2018), Journal of Petrology, doi: 10.1093/petrology/egy025

Thomas M. Gernon [1]*, R. Stephen J. Sparks[2], Matthew Field[3], Rachael Ogilvie-Harris[2], John C. Schumacher[4] and Richard Brooker[2]

[1]School of Ocean and Earth Science, University of Southampton, European Way, Southampton SO14 3ZH, UK; [2]School of Earth Sciences, University of Bristol, Wills Memorial Building, Queens Road, Bristol BS8 1RJ, UK; [3]Wood PLC, Mining & Minerals, 12th Floor Canada Square, Canary Wharf, London E14 5LQ, UK; [4]Department of Geology, Portland State University, 1721 SW Broadway Ave, Portland, OR 97207, USA

*Corresponding author. School of Ocean and Earth Science, University of Southampton, European Way, Southampton SO14 3ZH, UK. Telephone: +44 (0) 23 8059 2670. Fax: +44 (0) 23 8059 3059. E-mail: thomas.gernon@noc.soton.ac.uk

Received July 5, 2018; Accepted December 9, 2018

Key words: kimberlite; geochemistry; phlogopite; xenolith; Snap Lake

Fulop *et al.* (2018) infer that the Snap Lake kimberlite intrusion (NWT Canada) was emplaced as a single batch of magma and that its internal variations are a consequence of alteration and interactions with granitoid host-rocks by deuteric fluids. However, field, petrological, geochemical and theoretical constraints support the involvement of multiple magma batches and show that the deuteric alteration hypothesis is implausible. Rather we propose that alteration is primarily the consequence of reactions between the kimberlite, country-rock xenoliths and surrounding granite with groundwaters during cooling and serpentinization at temperatures between 400°C and ambient.

Fulop *et al.* (2018) present new data for the Snap Lake kimberlite intrusion in which they interpret variations in mineral assemblages and bulk-rock geochemistry as the consequence of alteration exclusively by deuteric fluids (i.e. late-stage magmatic fluids related to solidification), combined with interaction between the kimberlite magma and granite host-rocks and xenoliths. They question the interpretation of previous studies (Field *et al.*, 2009; Gernon *et al.*, 2012) that there are marked compositional variations of igneous origin in the parental kimberlite magma, leading to primary zoning within the intrusion. While these kimberlites are indeed profoundly altered, the main new interpretations require implausible amounts of magmatic fluids to be transported with the kimberlite magma (Brooker *et al.*, 2011). Further, this hypothesis is not consistent with the observed alteration mineral assemblages, which we show here, were formed at low temperature by very water-rich fluids. Observations at Snap Lake can be largely explained by compositional variations in the kimberlite overprinted by alteration (predominantly serpentinization) by groundwater. However, some features of these rocks could have originated by reactions between melts, fluids, primary igneous crystals and entrained xenoliths during the initial stages of solidification.

Fulop *et al.* (2018) discredited our earlier studies making the incorrect statement that Gernon *et al.* (2012) 'mapped [rock types] from underground photographs'. In reality, field data and observations were collected underground at Snap Lake with De Beers Canada geologists over several months (2008–2009), using well-established underground mapping techniques and direct observations of rock faces. In 2008–2009 Gernon *et al.* (2012) mapped approximately 1500 m of underground faces (equating to an area of $>4500\,m^2$) covering the spatial footprint of the mine (see figure 1e and supplementary material in Gernon *et al.*, 2012). A total

of 40 representative samples were extracted at regular intervals across the mine and from drill cores. High-resolution oriented photographs of rock faces were used only for image analysis of key parts of the dyke (see Field *et al.*, 2009; Gernon *et al.*, 2012). As the underground mine workings were flooded after closure of the Snap Lake Mine in 2015, we revisit data and detailed field and petrographic observations that formed the basis of the studies by Field *et al.* (2009), Gernon *et al.* (2012) and Ogilvie-Harris (2012).

In this *Comment*, we address three topics: (1) the implausibility of magmatic fluids being the main cause of alteration; (2) the evidence that variations across the intrusion have a magmatic signature and cannot be explained entirely by alteration; and (3) a model of largely low temperature alteration caused by reaction of the fluids generated by serpentinization with acidic cratonic groundwaters and brines, which overprints the primary variations related to igneous processes.

ALTERATION: FLUID SOURCES AND CONDITIONS

To be absolutely clear we are not claiming that there was no deuteric alteration. Following and during dyke emplacement there will have been a brief period of cooling and crystallization, during which there could have been reactions between the dyke's constituents (primary crystals, melts, magmatic fluids and entrained xenoliths). However, here we show that any reactive fluids generated at this stage cannot be the main source of fluid that caused the predominant alteration.

The presence of igneous phlogopite in the Snap Lake intrusion indicates that the kimberlite magma was hydrous, so the central question is whether the amount of water transported by the kimberlite into the location of emplacement could account for the alteration. The main alteration products (serpentine and phyllosilicates) require a large amount of water to have been transported. In order to constrain the amount of water, it is necessary to know the depth of dyke emplacement, the solubility of water in the melt and the porosity of the magma, developed during and perhaps shortly after emplacement. Here we estimate an upper bound on this amount.

The depth of emplacement is well constrained by (U–Th)/He age dating of zircons and apatites (Flowers *et al.*, 2006) which demonstrate very long-lived stability of the Canadian shield with no more than 1·5–2 km of erosion from mid-Proterozoic times (note the intrusion is exposed underground at 280 to 320 m elevation, ~100 to 150 m below the present-day surface). Thus, we used a lithostatic pressure of 20 MPa for a maximum depth of 2 km, plus 10 MPa for the typical overpressures associated with dyke emplacement, for our calculations. The solubility of water in kimberlite melts is constrained by experimental studies (Brooker *et al.*, 2011) and is thought to be very similar to that in basaltic melts (i.e. ~2–3 wt % at 30 MPa; Moussallam *et al.*, 2016). Based on the Snap Lake mineralogy (olivine, monticellite, phlogopite, oxides and minor carbonate) we assume a dissolved water content of 2·0 wt %, using experimentally constrained solubility laws. Using a magma temperature of 800°C constrained by low-pressure phlogopite stability (Righter & Carmichael, 1996), the density of water at 30 MPa is about 50 kg/m^3. Assuming a conservative magma porosity of 10% and a magma density (crystals plus melt) of 2750 kg/m^3, then 0·2 wt % could be transported as an exsolved phase. There is however a trade off in that the higher the porosity the lower the melt fraction, so the total exsolved and dissolved water will decrease with increasing porosity. Phlogopite typically contains about 3·5 to 4 wt % water. The mode of phlogopite in some Snap Lake rocks exceeds 50%, suggesting a melt water content of at least 2 to 3%, consistent with the above calculations.

Now consider the water budget needed for alteration. Table 6 in Fulop *et al.* (2018) shows typical loss on ignition values of around 15 wt %. Given that much of the Snap Lake magma is highly porphyritic, the water would need to be carried in the melt, so the requirement is for the magma to transport 25–30 wt % water, an order of magnitude greater than what is plausible for magmatic water content. We conclude that another source for almost all the water is required. Given that the granite country rocks contain only minor amounts of water (0·1 to 0·4 wt % according to the modal data), groundwater is the only plausible source and we therefore dismiss the hypothesis that the alteration is largely deuteric (i.e. involving magmatic water).

Fulop *et al.* (2018) also invoke magmatic CO_2 in their reactions, with formation of dolomite as a by-product of serpentinization. It is hard to distinguish primary from secondary carbonates in such highly-altered rocks and we concur that primary kimberlite magmas are commonly carbonatitic in character (e.g. Russell *et al.*, 2012; Kamenetsky *et al.*, 2014). Thus, magmatic CO_2 might have played a role, but for the same reasons as argued for water, exsolved CO_2 cannot have supplied much mass for alteration. Alternatively, a decarbonation reaction of igneous carbonate may have occurred at magmatic temperatures to release magmatic CO_2. However, there is a simpler alternative explanation for the presence of abundant carbonate (notably in late-stage veins, Fig. 1) at Snap Lake that derives from the extensive literature on low-temperature serpentinization (e.g. Charlou *et al.*, 2002; Oze & Sharma, 2007). Serpentinization reactions change the fluids profoundly with respect to pH, oxidation state and composition (Palandri & Reed, 2004). Formation of carbonate is ubiquitous where very highly alkaline and highly reduced serpentinizing fluids mix with neutral or acidic external water (Palandri & Reed, 2004; Schrenk *et al.*, 2013), commonly moderated by microbial activity. Below we develop an interpretation in which serpentinization generates fluids that react with groundwater at the intrusion margins and in the near-field host-rock. A key point developed below is that the alteration mineral assemblages do not support involvement of a CO_2-rich fluid.

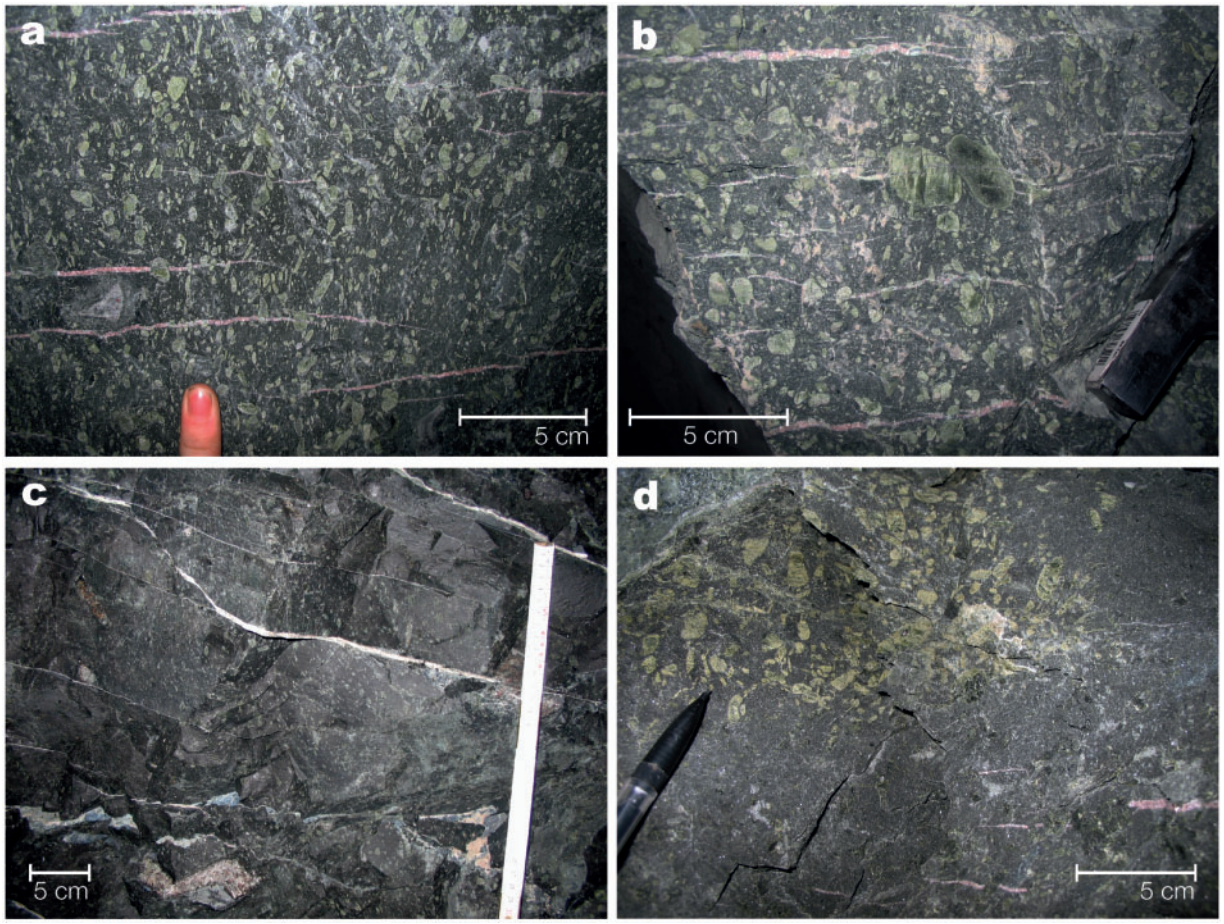

Fig. 1. Field photographs showing some characteristic features of Snap Lake kimberlites. (**a**) Olivine-rich macrocrystic kimberlite (ORK) showing a strong sub-vertical fabric defined by the alignment of elongate olivine macrocrysts. Note the dyke margins are roughly parallel to the calcite veins (i.e. sub-horizontal), so the fabric is developed perpendicular to the dyke margins. (**b**) ORK showing a high concentration of large olivine macrocrysts. (**c**) Kimberlite transitional between ORK and olivine-poor kimberlite (OPK), showing a patchy distribution, and relatively low abundance, of olivine macrocrysts. The scattered distribution of olivine indicates that the low olivine abundance is a primary feature, inconsistent with a deuteric alteration overprint (i.e. there is no reason why deuteric alteration would selectively pseudomorph some olivine macrocrysts, and completely evade adjacent olivine macrocrysts). (**d**) Cognate xenolith of ORK in OPK, showing sharply defined contacts (Field *et al.*, 2009). Note that olivine macrocrysts are visible in the OPK, but less abundant. Such features are hard to explain in the context of deuteric alteration, which invokes a gradational transition between ORK and OPK (Fulop *et al.*, 2018). In addition, a deuteric alteration overprint of OPK would need to selectively exclude many olivine macrocrysts, which remain intact (Figs 2 and 3). It is clear that all these rocks are pervasively altered (Gernon *et al.*, 2012).

One further difficulty for the deuteric hypothesis is that in a low angle (15°) dyke (almost a sill) the fluids escaping from the magma should move upwards. Thus, one might expect to observe much stronger alteration effects in the roof of the intrusion than the floor. Such asymmetric effects are not reported in this and previous studies of Snap Lake. Our detailed observations of mine sections (Field *et al.*, 2009; Gernon *et al.*, 2012) agree with the schematic sections (figures 2 and 3) in Fulop *et al.* (2018) that show the variations across the intrusion are symmetric. One possibility for generating symmetrical sections is if the magma intrusion had a high fluid (gas) overpressure, resulting in decompression and outflow of volcanic fluids. However, we have already shown that the amount released is far too small to cause the proposed alteration.

ORIGIN OF THE MINERALOGICAL AND GEOCHEMICAL VARIATIONS

The hypotheses that variations within the Snap Lake intrusion are the consequences of diverse magma compositions, of interaction among these magmas and country-rock, and alteration are not mutually exclusive. However, Fulop *et al.* (2018) adopt the position that the latter two processes can explain all the observations. Our intention here is to show unequivocally that there are primary magmatic variations, reiterating some of

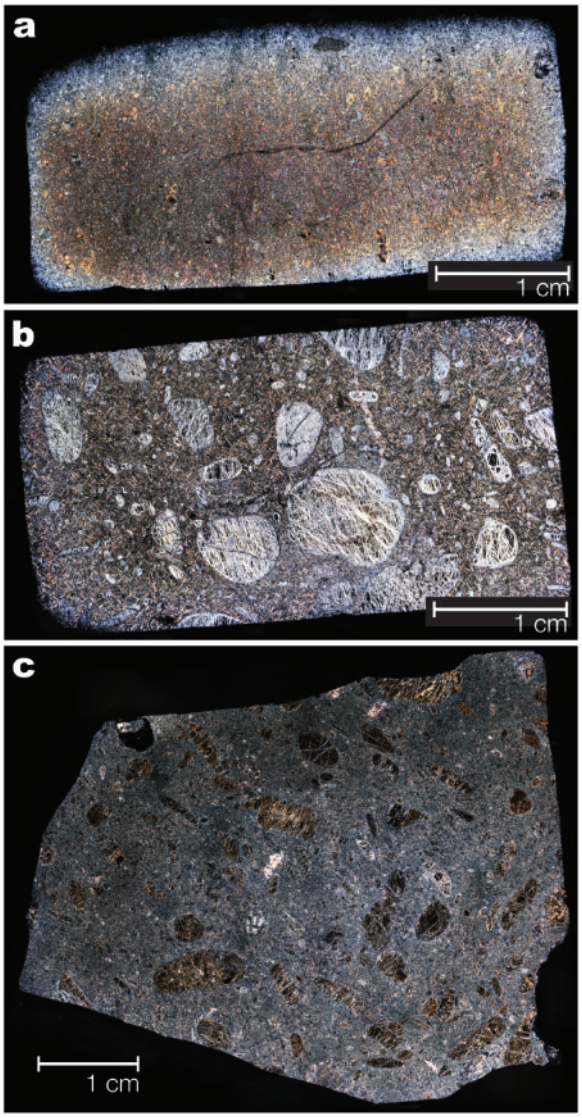

Fig. 2. Photomicrographs (transmitted light) of three main kimberlite lithofacies identified in Field *et al.* (2009) and Gernon *et al.* (2012). (**a**) Olivine-poor kimberlite (OPK). Olivine macrocrysts are heavily serpentinized, yet still visible, but sparse relative to the ORK. The deuteric alteration hypothesis of Fulop *et al.* (2018) requires that the abundance of olivine macrocrysts was originally equivalent to the ORK [see (**c**)], and these crystals have since been pseudomorphed by phyllosilicates. Small serpentinized olivines are visible, but the purported pseudomorphs are not (see also Fig. 3). (**b**) Transitional ORK–OPK variety studied by Field *et al.* (2009). Again, serpentinized olivine macrocrysts are clearly discernible. Note the abundance of platy phlogopite in the groundmass defining a decussate-like texture. (**c**) Olivine-rich kimberlite from sample S1 (Gernon *et al.*, 2012). Here, the modal abundance of olivine macrocrysts is much higher than that of the OPK, and there is significantly less phlogopite. Note the slightly smaller scale in (**c**).

the key observations already presented in Field *et al.* (2009) and Gernon *et al.* (2012), and drawing on some of the new data presented by Fulop *et al.* (2018).

Field observations and lithofacies variations

A key assertion by Fulop *et al.* (2018) is that the Snap Lake intrusion is comprised of a single magma and the internal variations reflect differences in alteration between the margins and centre, with replacement of abundant olivine and monticellite by serpentine and phyllosilicates, including phlogopite. However, there are several marked differences in the characteristics of the marginal and central rocks. First there is a significant difference in olivine size and abundance, clearly evident in figures 4 and 5 of Fulop *et al.* (2018), as well as in the data presented by Gernon *et al.* (2012).

Figures 1 and 2 show contrasted macroscopic textures observed in olivine-rich kimberlite (ORK) and olivine-poor kimberlite (OPK). Gernon *et al.* (2012) stress that the Snap Lake kimberlites are pervasively altered and that this alteration varies in style: in some areas, olivine is replaced by pale (low-Mg) serpentine and in others by dark (high-Mg) serpentine. Even where differential alteration has occurred, olivine macrocrysts are discernible, and their abundance varies locally to define olivine-rich and olivine-poor regions (Fig. 1). In some areas, a uniformly scattered distribution of olivine is observed (Fig. 1c), which would not be expected if the intergranular kimberlite formed as a result of deuteric alteration. The ORK crystals show a strong sub-vertical fabric (Fig. 1a) that is not developed in the OPK (figures 3 and 4 in Gernon *et al.*, 2012), pointing to fundamental differences in the magmatic emplacement of these lithofacies.

Fulop *et al.* (2018) argue that the changes from HK1 (defined as ORK in our previous publications) to HK6 (OPK) are always gradational. However, they only provide photographs of discrete core samples (rather than outcrop-scale relationships), making the evidence for a gradual transition unclear to the reader. Field *et al.* (2009) and Gernon *et al.* (2012) show that abrupt changes between varieties are common (e.g. Fig. 1d), and occur at all levels in the dyke. Both gradual and abrupt changes can occur during magma mingling, so these gradual variations are not convincing evidence for an alteration model (but alteration might well lead to more diffuse contacts).

Olivine and phlogopite textures

Fulop *et al.* (2018) describe textures from which they infer replacement of olivine macrocrysts by phlogopite and other phyllosilicates. We do not find them convincing; their approach of drawing a bold red outline (e.g. their figure 7) obscures the supposed boundary of the pseudomorph. Rather, the textures of the OPK (see Fig. 2), observed under Scanning Electron Microscope (SEM), are inconsistent with a deuteric alteration overprint as now demonstrated. The images (Fig. 3a–e) are taken from OPK at the top of the profiles ND1-01 and ND2-06 shown in Field *et al.* (2009) and Gernon *et al.* (2012). First, olivines are present as discrete macrocrysts, with little evidence for phyllosilicate replacement or substitution pseudomorphing (Fig. 3). Second, there are many quite abrupt contacts between phlogopite and olivine (Fig. 3b–d), and the phlogopite laths are

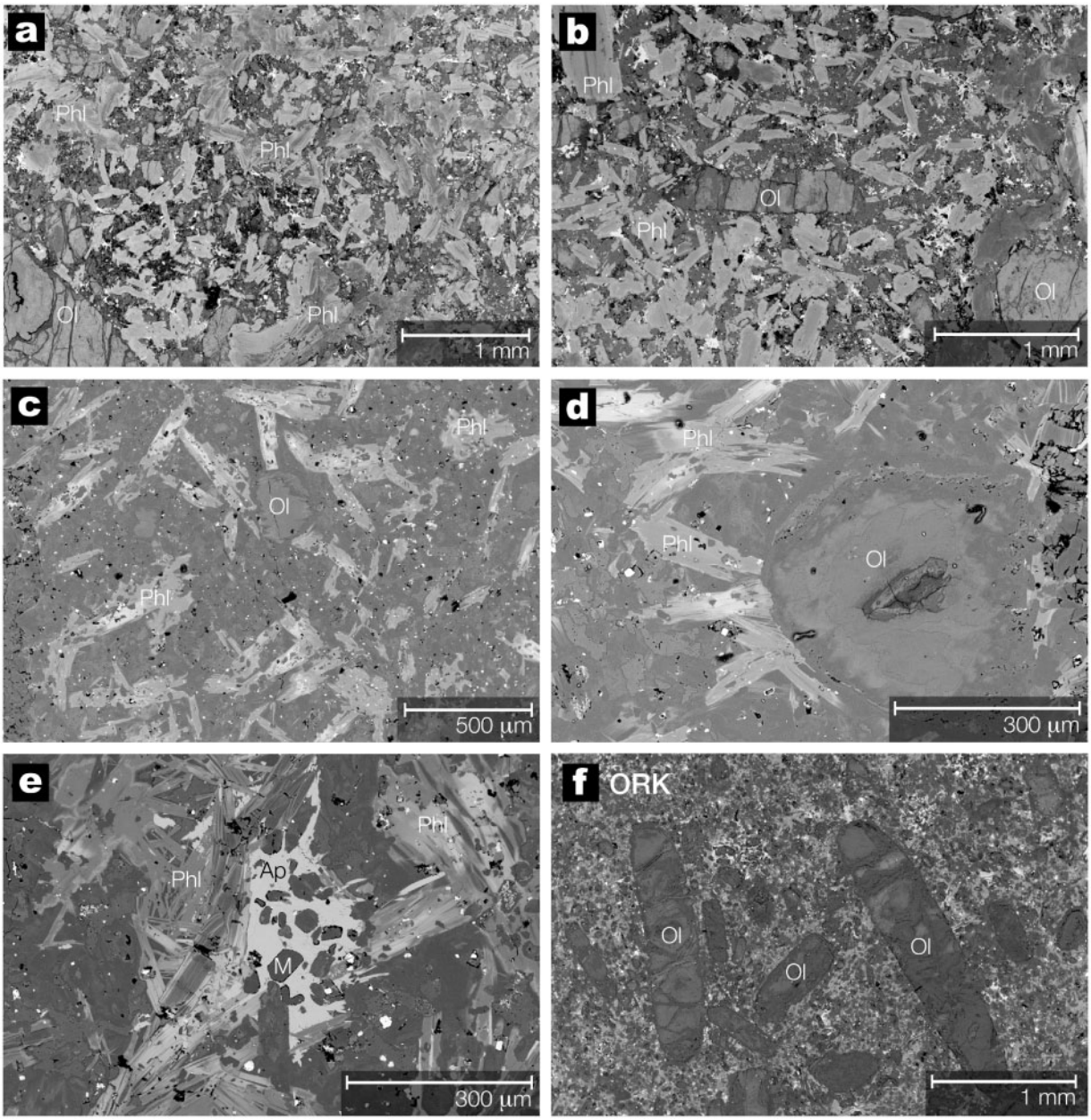

Fig. 3. SEM photomicrographs of OPK from Snap Lake. (**a**) and (**b**) OPK from the top of profile ND2-06 (Field *et al.*, 2009; Gernon *et al.*, 2012). Here, olivine occurs as discrete macrocrysts. The phlogopite laths are randomly orientated and do not appear to be pseudomorphing olivine macrocrysts [compare with ORK shown in (**f**)]. (**c**) OPK from the top of profile ND1-01, showing randomly oriented phlogopite laths, some of which abruptly terminate at olivine crystal boundaries. (**d**) OPK from the top of profile ND1-01; again the phlogopite does not pseudomorph olivine macrocrysts, but rather terminates abruptly at their outer boundaries (i.e. inconsistent with pseudomorphing). (**e**) OPK from the top of profile ND1-01; here apatite poikilitically encloses serpentinized monticellite and adjacent phlogopite, indicating that these are early-formed crystals. (**f**) For comparison, ORK showing a characteristic fabric defined by olivine macrocrysts (Gernon *et al.*, 2012). Abbreviations: Phl, phlogopite; Ol, olivine; M, monticellite; Ap, apatite.

randomly orientated (Fig. 3a–d), reminiscent of decussate textures. Fulop *et al.* (2018) accept that the 'random, cross-cutting orientations' of phlogopite evidence late-stage crystallization from a magma (*sensu* Gernon *et al.*, 2012). Third, serpentinized monticellite is found poikilitically enclosed in apatite (Fig. 3e). The apatite clusters appear to grow up to the edges of (and partially enclose) the phyllosilicates (Fig. 3e), suggesting the latter are not late replacement features. Fourth, the overall distribution of phyllosilicates (e.g. ND2-06a, Fig. 3a) is not at all reminiscent of the textures and crystal size distribution defined by olivine in ORK (e.g. Fig. 3f), which Fulop *et al.* (2018) argue to be the OPK 'protolith.' Finally, many phlogopites exhibit lath-like geometries and are surrounded by serpentine groundmass, with the latter associated with other primary

kimberlite minerals such as spinel and titanite. Such textures cannot be generated by overprinting olivine macrocrysts and microcrysts.

Diamond and olivine distributions

We present several lines of evidence that the petrological and mineralogical characteristics of ORK and OPK are related to primary magmatic variations. We disagree with Fulop *et al.* (2018) that diamond distributions are the critical variable in interpreting the number of kimberlite magma batches involved: diamonds are xenocrysts in kimberlite and are included by chance during magma ascent from the mantle. Therefore, it is equally probable that one batch of magma might sample the same portion of the mantle as a second. Consequently, the petrological and mineralogical characteristics must be considered the first-order factors in resolving the emplacement phases.

Field *et al.* (2009) recovered bulk samples from the ORK and OPK lithofacies (Gernon *et al.*, 2012), ranging from 30 to120 tonnes (averaging 60 tonnes) in mass. Sampling on this scale is essential to make a representative assessment of diamond grade (Rombouts, 2003) and distribution across a range of diamond sizes. Ore extraction during bulk sampling was very carefully supervised to mitigate contamination of different lithofacies. Field *et al.* (2009) demonstrate that the diamond and olivine grain sizes at Snap Lake are positively correlated and show clear differences in the diamond and olivine distributions for OPK and ORK (Fig. 4). This corroborates multi-phase emplacement, but is not essential evidence (Gernon *et al.*, 2012). Field *et al.* (2009) also show that the cumulative average diamond size varies laterally in the intrusion and is strongly correlated with lateral lithofacies variations. The cumulative average diamond size is lowest in areas that are dominated by OPK (figure 9, Field *et al.*, 2009), and highest in ORK-dominated regions of the dyke.

Fulop *et al.* (2018) present microdiamond data showing that the different lithofacies are almost identical (their figure 17), but larger diamonds show significant and systematic variations (Field *et al.*, 2009). This difference could be explained by the widespread sampling strategy (i.e. combining samples from different locations, leading to mixing of lithofacies; see their figure 1), and the relatively small sample size (175 × 8 kg samples) employed by Fulop *et al.* (2018).

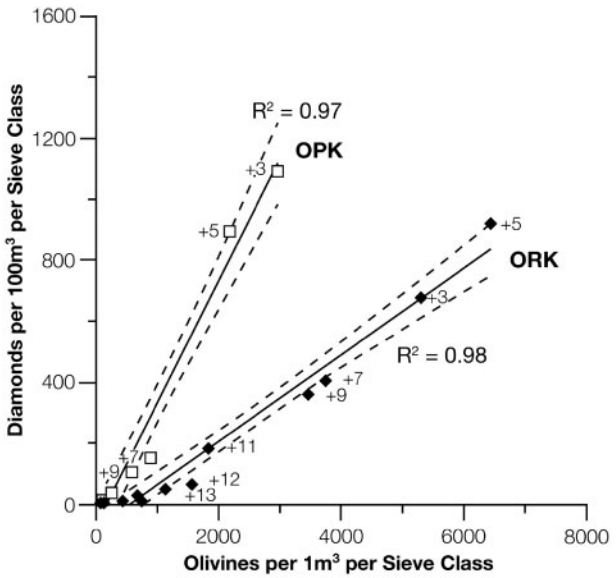

Fig. 4. A comparison of the proportions of olivine and diamond retained for different DTC sieve classes for ORK (black diamonds) and OPK (white squares). The dashed lines signify 95% confidence intervals around fitted linear distributions (after Field *et al.*, 2009). A linear correlation is evident for both lithofacies, which are distinct in terms of diamond distributions.

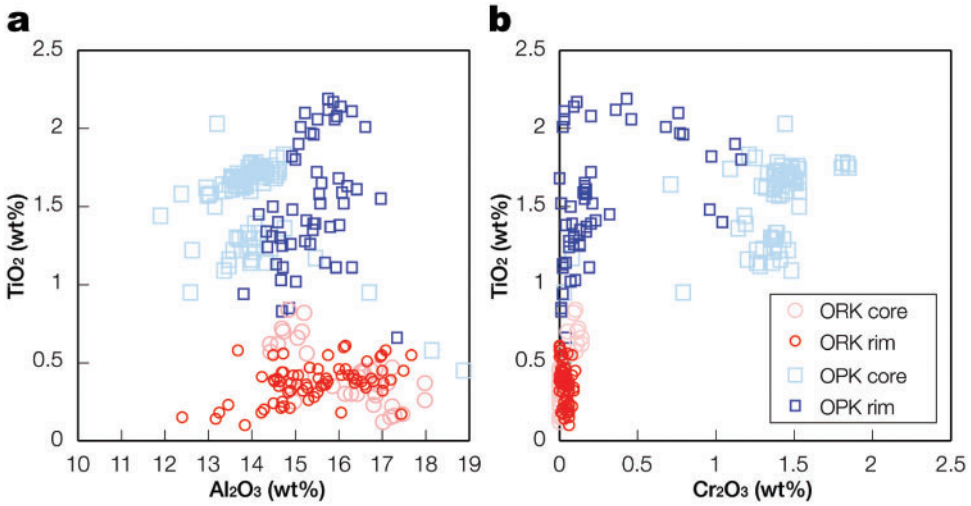

Fig. 5. The defining chemical characteristics of OPK and ORK phlogopites and the general core-rim trends for TiO_2 plotted against (**a**) Al_2O_3 and (**b**) Cr_2O_3.

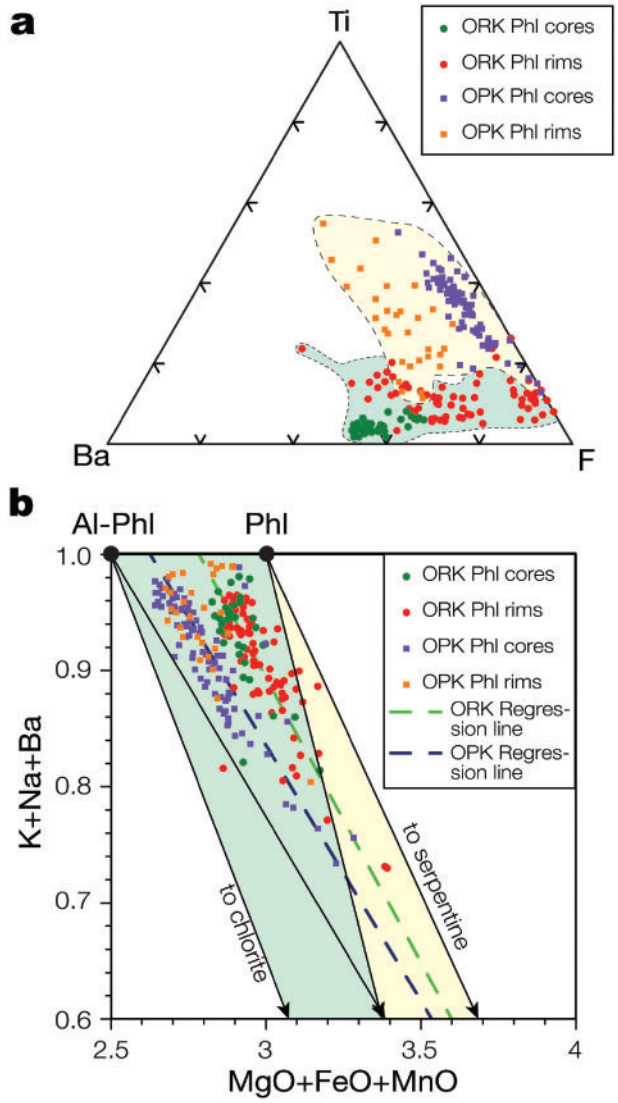

Fig. 6. (**a**) Ternary plot of apfu values for Ba, F and Ti for phlogopite and partially altered phlogopite analyses from olivine-poor (OPK) and olivine-rich (ORK) kimberlite as defined by Field *et al.* (2009) and Gernon *et al.* (2012). Pale-green field encloses analysis points from the ORK; pale-yellow field encloses analysis points from the OPK. **(b)** Plot of sheet-silicate interlayer cations K+Na+Ba vs divalent octahedral cations Mg+Fe^{2+}+Mn for phlogopite and partially altered phlogopite analyses from the OPK and ORK. Filled black circles: end-member phlogopite (Phl) and eastonitic phlogopite (Al-Phl) ($KMg_{2.5}Al_{0.5}Si_{2.5}Al_{1.5}O_{10}(OH)_2$). Arrows show mixing lines to end-members of chlinochlore ($Mg_{3.929}Al_{0.786}Si_{2.357}Al_{0.786}O_{11}$) and serpentine ($Mg_{4.714}Si_{3.143}O_{11}$), both recalculated to an anhydrous 11 oxygen cation basis. Dashed lines: reduced-major axis regression lines for phlogopite and partially altered phlogopite analyses from the OPK and ORK.

Phlogopite chemistry

The marginal rocks are richer in phlogopite and poorer in serpentinized olivine, based on modal data and bulk-rock geochemistry (higher K and lower MgO), and occupy distinctive fields in figure 15 of Fulop *et al.* (2018). In contrast to Fulop *et al.* (2018), we found phlogopite-rich margins in the area with metavolcanic country-rock (see figure 3 in Gernon *et al.*, 2012). We interpret these relationships as due to a variation in the melt compositions from which the phlogopite precipitated.

We find clear differences between the OPK and ORK phenocrystal (matrix) phlogopites, reflected in their TiO_2 and Cr_2O_3 contents (Fig. 5). ORK phlogopite ranges between 0·85 and 2·2 wt % TiO_2; whereas the OPK phlogopites have a lower range between 0·10 and 0·85 wt % TiO_2 (Fig. 5). The Cr_2O_3 contents are very low in the ORK (0–0·2 wt %) and show a considerably wider range in the OPK (0–2 wt %). Similarly, Kopylova *et al.* (2010) showed the presence of low (0·1–0·5 wt %) and high (1–1·6 wt %) Cr_2O_3 phlogopites at Snap Lake, yet Fulop *et al.* (2018) did not measure Cr_2O_3 during phlogopite analysis (see supplementary file EST1 in their paper). Indeed Cr_2O_3 content is regarded as an important petrogenetic indicator in kimberlites (Reguir *et al.*, 2009; Sobolev *et al.*, 2009; Soltys *et al.*, 2018). It must be stressed that not all elements will respond in exactly the same way to alteration, since high field strength elements tend to be less mobile. Other elements in the phlogopite analyses support division into ORK and OPK magmas. For example, a ternary plot of apfu values for Ba, F, and Ti (Fig. 6a) shows distinct fields for the OPK and ORK, as well as for the cores and rims of each type; cores of OPK phlogopites have lower Ba contents than cores of ORK phlogopites.

Fulop *et al.* (2018) state that >60% of all analysed phlogopite grains from Snap Lake are actually submicroscopic mixtures of several phyllosilicates, including serpentine. Their primary concern is analysis points that depart from an inverse 1:1 or 1:2 relationship on plots of K versus Ba (figure 3 in Fulop *et al.*, 2019). A plot of total interlayer site cations (K, Na, Ba) vs divalent octahedral cations (Mg, Fe^{2+}, Mn) can help identity the phase(s) causing the interlayer site deficiencies. On the plot (Fig. 6b), ideal Mg-end members for talc, clinochlore and serpentine lie at 0·000 K and at 3·000, 3·929, and 4·714 Mg (based on 11 oxygen atoms, anhydrous), respectively. Phlogopite and eastonitic phlogopite ($KMg_{2.5}Al_{0.5}$ $Si_{2.5}Al_{1.5}O_{10}(OH)_2$) plot at 1·000 K and at 3·000 and 2·500 Mg, respectively (Fig. 6b). On this plot, the OPK and the ORK phlogopite analyses form two distinct elongate groups. Reduced-major axis regression lines through each of the groups intercept the 0·0 K+Na+Ba axis at Mg+Fe^{2+}+Mn values of 4·823 and 4·898, very close to the ideal value for serpentine (4·714) and strongly suggest the phlogopites have undergone some alteration to serpentine, consistent with Fulop *et al.* (2018). However, the observation that the OPK and ORK form two subparallel, elongate (Fig. 6b) arrays indicates that the eastonite components of the pre-alteration compositions of these phlogopites were different. This feature shows that, despite the alteration, phlogopites preserve indicators of their primary chemistry, which in turn further supports the interpretation that the phlogopites crystallized from magmas of different composition. Indeed, the textures shown by Fulop *et al.* (2018) (their figure 11b,c) are more consistent with resorption and regrowth (cf. O'Brien *et al.*, 1988) and typical of cases where magma

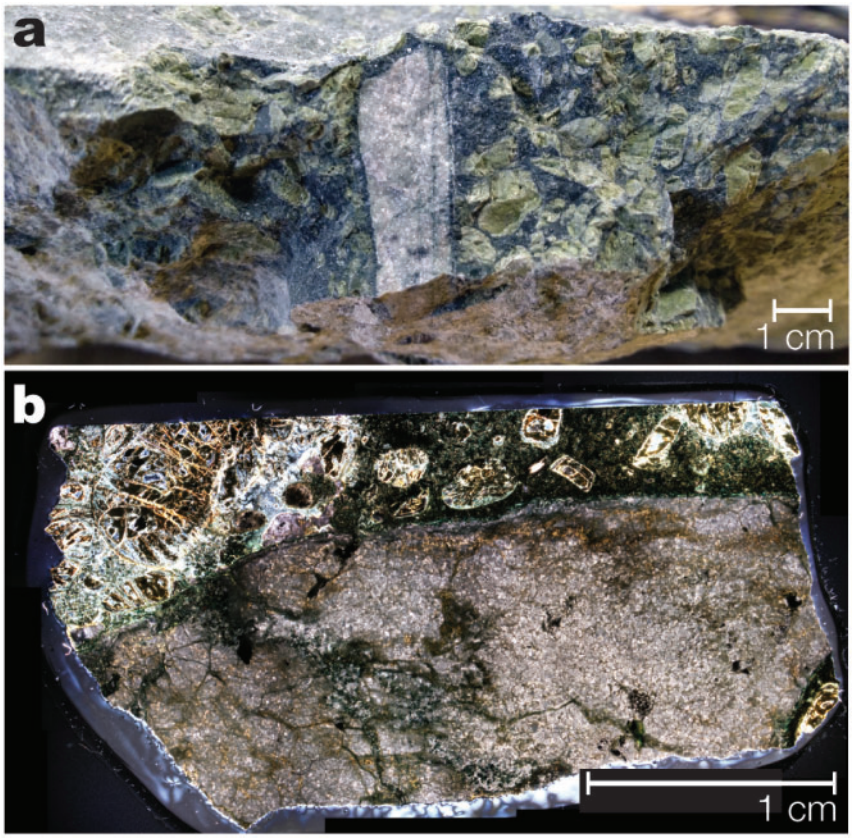

Fig. 7. (**a**) Photograph of a granitoid lithic clast recovered near the upper intrusion contact, showing sharp boundaries and local concentrations of olivine macrocrysts. (**b**) Thin section of a granite clast showing a sharp boundary with the adjacent kimberlite, a phyllosilicate-rich 'halo' is not discernible.

recharge or convection through a temperature gradient have been proposed.

Problems with isocon analysis in kimberlite studies

The isocon method used by Fulop *et al.* (2018) is problematic in kimberlites because it requires: (a) access to an unaltered sample and (b) that the compositions of the rocks were originally the same (Grant, 1986; Guo *et al.*, 2009). Fulop *et al.* (2018) assume that kimberlites in the centre of the dyke (i.e. HK1) are 'fresh,' but these too are heavily serpentinized (Field *et al.*, 2009; Gernon *et al.*, 2012). Using this method they also needed to assume that HK1 is the protolith of HK6, so circular reasoning is employed. There are further complications in using 'average fresh granitoid' (tonalite with $K_2O < 2$ wt %) as the granite protolith, because the country rocks of the Defeat pluton suite (2·61–2·59 Ga) exposed in this region are highly heterogeneous (banded on a cm–m scale), comprising granodiorite, tonalite and monzogranite, with muscovite-bearing pegmatites locally (Stubley, 2000). Grant (1986) and Guo *et al.* (2009) stress that the isocon approach requires progressively altered samples and the starting material must be near identical for such normalisation methods to produce valid results.

Granitoid clasts and assimilation

Fulop *et al.* (2018) speculate that locally-derived xenoliths can interact with magmas. They also suggest that granitic xenoliths are partially digested in the melt, contributing to local increases in Si and Al in the kimberlite and identify 'haloes' enriched in phlogopite around granitoid xenoliths (see figures 5 and 9 in Fulop *et al.*, 2018). However they do not show convincing evidence of partially digested granite clasts from this kimberlite. We find that granite clasts within the intrusion are angular (i.e. not consistent with partial digestion) and directly in contact with olivines, with negligible phyllosilicate enrichment (e.g. Fig. 7).

There are difficulties for low temperature kimberlite magmas assimilating highly refractory granitic rocks. Although not accurately constrained, estimates of kimberlite magma temperatures are around 800°C, at shallow crustal depths; experimental studies indicate that at low pressure (20 MPa) phlogopite will not be stable above 900°C (Wones & Eugster, 1965; Righter & Carmichael, 1996). Granites are, however, very refractory because of their low water contents. A very small amount of melt should be formed at <900°C due to biotite breakdown, but temperatures typically need to exceed 1000°C for significant melting of granite xenoliths (e.g. Tuttle & Bowen, 1958) and about 1100°C for

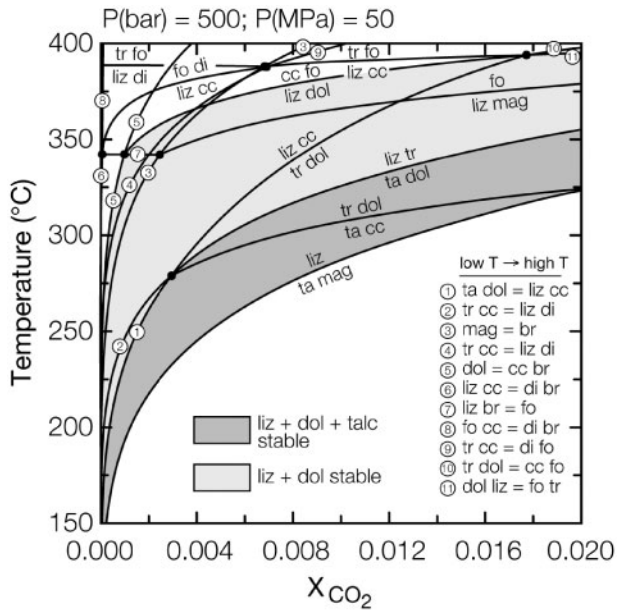

Fig. 8. T–XCO_2 diagram of stable phases for the system CaO–MgO–SiO_2–H_2O–CO_2. Calculations assume saturation with an H_2O–CO_2 fluid using the Perple X application suite (Connolly, 2005) and the Holland & Powell (2004) thermodynamic database (hp02ver.dat) modified by Connolly & Kerrick (2002). Abbreviations: br, brucite; cc, calcite; di, diopside; dol, dolomite; fo, forsterite; liz, lizardite; ta, talc; tr, tremolite. Al-free chlorite (afchl), which has the same mineral structure and composition as Al-free lizardite, was used as 'lizardite' in the calculations. Reactions with wollastonite and quartz are also stable, but do not bear on this discussion and were left off the diagram to improve clarity.

tonalite. Therefore, thermodynamically it is problematic to digest granitoid clasts in a kimberlite melt at these shallow crustal depths.

It is also important to consider heat transfer to the walls of the intrusion (Sparks *et al.*, 2006) and the cooling effects of lithic clasts (typically 10–20 vol.%, and locally up to 40 vol.% at Snap Lake; Gernon *et al.*, 2012), which could reduce the magma temperature by 300–400°C (Pell *et al.*, 2015), inhibiting granitoid assimilation. A simpler explanation for elevated mineral concentrations around some lithic clasts are thermal processes (e.g. quenching around cold clasts), or fluid dynamic phenomena such as flow alignment, which is common in magmas with such high crystal concentrations (Smith, 2000).

Mineral stability

Finally, we consider the stability of alteration phases reported in the Snap Lake kimberlite. Figure 8 is a T–XCO_2 diagram at 50 MPa like the one cited by Fulop *et al.* (2018), but calculated using a different thermodynamic dataset (Holland & Powell, 2004). The diagram shows that all the alteration assemblages and proposed reactions only occur at temperatures below 400°C and indeed can occur at much lower temperatures approaching ambient. On this basis, the figure excludes a deuteric origin for the assemblages. Fulop *et al.* (2018) suggest that the lack of perovskite and primary calcite in parts of the dyke is the result of deuteric alteration through the reaction:

$$2{\cdot}Mg_2SiO_4 + CaCO_3 + CO_2 + 2{\cdot}H_2O = Mg_3Si_2O_5(OH)_4 + CaMg(CO_2)_2 \quad (1)$$

Ca-depletion is attributed to this reaction, but this reaction causes Ca to be redistributed among minerals rather than lost from the system. Figure 8 shows that reaction 1 is encountered only for very water-rich fluids (c. 98·2–99·9% H_2O) and temperatures ranging from about 340–380°C. These temperatures mark the upper limit of dolomite + serpentine (lizardite), minerals either observed or reported from X-ray powder diffraction results (tables 2 and 3, Fulop *et al.*, 2018). The assemblage: serpentine (liz) + dolomite + talc (tables 2 and 3, Fulop *et al.*, 2018) is restricted to temperatures below about 340°C, depending on fluid composition (Fig. 8). For essentially pure H_2O fluids both these assemblages could be stable at temperatures less than 150°C. Thus, we infer that alteration of the dyke resulted from influx and interaction with groundwater during and after cooling. Consistent with this, stable isotope (i.e. $\delta_{18}O$ and $\delta_{13}C$) compositions of kimberlites in a global compilation, coupled with isotopic modeling (Giuliani *et al.*, 2014), strongly indicate that serpentine cannot crystallize from deuteric fluids, and copious amounts of externally-derived water are required (see Sparks, 2013).

Geochemical modification of the adjacent granites described by Fulop *et al.* (2018) can also be explained by relatively low temperature alteration by serpentinizing fluids. In other geological contexts, alteration of country rocks in contact with serpentinites results in rodingitization, which in granites can involve local Ca and Mg-metasomatism and result in Si, K and Na depletion (Wares & Martin, 1980; Normand & Williams-Jones, 2007). There is no necessity to invoke higher temperature magmatic interactions to explain the observations.

ALTERATION MODEL

It is useful to recognize two stages in the alteration history of Snap Lake. The first stage takes place during emplacement and cooling of the intrusion. Its duration will be short and is controlled by heat loss, crystallization and penetration of groundwater into the intrusion, resulting in the onset of alteration. For an intrusion 4 m thick, the conductive cooling time is estimated as less than 60 days using a thermal diffusivity of $8 \times 10^{-7} m^2 s^{-1}$ (Gernon *et al.*, 2012). The second stage occurs after the cooling of the intrusion is complete, and in principle could be 537 million years (i.e. since emplacement;

Agashev *et al.*, 2008), although we think it likely that alteration was complete in much less time than this. Summarising the above evidence and arguments, deuteric alteration can be ruled out and the alteration of the kimberlite and granitoid host rocks can be explained by serpentinizing groundwaters.

Severe alteration is the most characteristic feature of kimberlites and overprints many of the magmatic stage features. In order to infer magmatic history, the alteration history must first be unraveled. Fulop *et al.* (2018) start from the assumption that many textures and mineral assemblages are magmatic in origin, unless proven otherwise. In other areas of petrology, the approach is that textures and features in highly altered rock are the consequence of alteration unless proven otherwise.

REFERENCES

Agashev, A. M., Pokhilenko, N. P., Takazawa, E., McDonald, J. A., Vavilov, M. A., Watanabe, T. & Sobolev, N. V. (2008). Primary melting sequence of a deep (>250 km) lithospheric mantle as recorded in the geochemistry of kimberlite–carbonatite assemblages, Snap Lake dyke system, Canada. *Chemical Geology* **255**, 317–328.

Brooker, R. A., Sparks, R. S. J., Kavanagh, J. L. & Field, M. (2011). The volatile content of hypabyssal kimberlite magmas: some constraints from experiments on natural rock compositions. *Bulletin of Volcanology* **73**, 959–981.

Charlou, J. L., Donval, J. P., Fouquet, Y., Jean-Baptiste, P. & Holm, N. (2002). Geochemistry of high H_2 and CH_4 vent fluids issuing from ultramafic rocks at the Rainbow hydrothermal field (36°14N, MAR). *Chemical Geology* **191**, 345–359.

Connolly, J. A. D. (2005). Computation of phase equilibria by linear programming: a tool for geodynamic modeling and its application to subduction zone decarbonation. *Earth and Planetary Science Letters* **236**, 524–541.

Connolly, J. A. D. & Kerrick, D. M. (2002). Metamorphic controls on seismic velocity of subducted oceanic crust at 100–250 km depth. *Earth and Planetary Science Letters* **204**, 61–74.

Field, M., Gernon, T. M., Mock, A., Walters, A., Sparks, R. S. J. & Jerram, D. A. (2009). Variations of olivine abundance and grain size in the Snap Lake kimberlite intrusion, Northwest Territories, Canada: a possible proxy for diamonds. *Lithos* **112**, 23–35.

Flowers, R., Bowring, S. & Reiners, P. (2006). Low long-term erosion rates and extreme continental stability documented by ancient (U–Th)/He dates. *Geology* **34**, 925.

Fulop, A., Kopylova, M., Kurszlaukis, S., Hilchie, L., Ellemers, P. & Squibb, C. (2018). Petrography of Snap Lake kimberlite dyke (Northwest Territories, Canada) and its interaction with country rock granitoids. *Journal of Petrology* **59**, 2493–2518.

Fulop, A., Kopylova, M., Kurszlaukis, S., Hilchie, L. & Ellemers, P. (2019). A Reply to the Comment by Gernon et al. on the "Petrography of the Snap Lake kimberlite dyke (Northwest Territories, Canada) and its interaction with country rock granitoids" by Fulop et al. (2018). *Journal of Petrology* **60**, 661–671.

Gernon, T. M., Field, M. & Sparks, R. S. J. (2012). Geology of the Snap Lake kimberlite intrusion, Northwest Territories, Canada: field observations and their interpretation. *Journal of the Geological Society* **169**, 1–16.

Giuliani, A., Phillips, D., Kamenetsky, V. S., Fiorentini, M. L., Farquhar, J. & Kendrick, M. A. (2014). Stable isotope (C, O, S) compositions of volatile-rich minerals in kimberlites: a review. *Chemical Geology* **374–375**, 61–83.

Grant, J. A. (1986). The isocon diagram; a simple solution to Gresens' equation for metasomatic alteration. *Economic Geology* **81**, 1976–1982.

Guo, S., Ye, K., Chen, Y. & Liu, J.-B. (2009). A normalization solution to mass transfer illustration of multiple progressively altered samples using the isocon diagram. *Economic Geology* **104**, 881.

Holland, T. J. B. & Powell, R. (2004). An internally consistent thermodynamic data set for phases of petrological interest. *Journal of Metamorphic Geology* **16**, 309–343.

Kamenetsky, V. S., Golovin, A. V., Maas, R., Giuliani, A., Kamenetsky, M. B. & Weiss, Y. (2014). Towards a new model for kimberlite petrogenesis: evidence from unaltered kimberlites and mantle minerals. *Earth-Science Reviews* **139**, 145–167.

Kopylova, M. G., Mogg, T. & Scott Smith, B. (2010). Mineralogy of the Snap Lake kimberlite, Northwest Territories, Canada, and compositions of phlogopite as records of its crystallization. *The Canadian Mineralogist* **48**, 549.

Moussallam, Y., Morizet, Y. & Gaillard, F. (2016). H_2O–CO_2 solubility in low SiO_2-melts and the unique mode of kimberlite degassing and emplacement. *Earth and Planetary Science Letters* **447**, 151–160.

Normand, C. & Williams-Jones, A. E. (2007). Physicochemical conditions and timing of rodingite formation: evidence from rodingite-hosted fluid inclusions in the JM Asbestos mine, Asbestos, Québec. *Geochemical Transactions* **8**, 1–19.

O'Brien, H. E., Irving, A. J. & McCallum, I. S. (1988). Complex zoning and resorption of phenocrysts in mixed potassic mafic magmas of the Highwood Mountains, Montana. *American Mineralogist* **73**, 1007–1024.

Ogilvie-Harris, R. C. (2012). Constraining the nature of kimberlite melts by textural, compositional and experimental methods. Ph.D. thesis, University of Bristol.

Oze, C. & Sharma, M. (2007). Serpentinization and the inorganic synthesis of H2 in planetary surfaces. *Icarus* **186**, 557–561.

Palandri, J. L. & Reed, M. H. (2004). Geochemical models of metasomatism in ultramafic systems: serpentinization, rodingitization, and sea floor carbonate chimney precipitation. *Geochimica et Cosmochimica Acta* **68**, 1115–1133.

Pell, J., Russell, J. K. & Zhang, S. (2015). Kimberlite emplacement temperatures from conodont geothermometry. *Earth and Planetary Science Letters* **411**, 131–141.

Reguir, E. P., Chakhmouradian, A. R., Halden, N. M., Malkovets, V. G. & Yang, P. (2009). Major- and trace-element compositional variation of phlogopite from kimberlites and carbonatites as a petrogenetic indicator. *Lithos* **112**, 372–384.

Righter, K. & Carmichael, I. S. E. (1996). Phase equilibria of phlogopite lamprophyres from western Mexico: biotite-liquid equilibria and P-T estimates for biotite-bearing igneous rocks. *Contributions to Mineralogy and Petrology* **123**, 1–21.

Rombouts, L. (2003). Assessing the diamond potential of kimberlites from discovery to evaluation bulk sampling. *Mineralium Deposita* **38**, 496–504.

Russell, J. K., Porritt, L. A., Lavallée, Y. & Dingwell, D. B. (2012). Kimberlite ascent by assimilation-fuelled buoyancy. *Nature* **481**, 352–356.

Schrenk, M. O., Brazelton, W. J. & Lang, S. Q. (2013). Serpentinization, carbon, and deep life. *Reviews in Mineralogy and Geochemistry* **75**, 575–606.

Smith, J. V. (2000). Textural evidence for dilatant (shear thickening) rheology of magma at high crystal concentrations. *Journal of Volcanology and Geothermal Research* **99**, 1–7.

Sobolev, N. V., Logvinova, A. M. & Efimova, E. S. (2009). Syngenetic phlogopite inclusions in kimberlite-hosted diamonds: implications for role of volatiles in diamond formation. *Russian Geology and Geophysics* **50**, 1234–1248.

Soltys, A., Giuliani, A. & Phillips, D. (2018). A new approach to reconstructing the composition and evolution of kimberlite melts: a case study of the archetypal Bultfontein kimberlite (Kimberley, South Africa). *Lithos* **304-307**, 1–15.

Sparks, R. S. J. (2013). Kimberlite volcanism. *Annual Review of Earth and Planetary Sciences* **41**, 497–528.

Sparks, R. S. J., Baker, L., Brown, R. J., Field, M., Schumacher, J., Stripp, G. & Walters, A. (2006). Dynamical constraints on kimberlite volcanism. *Journal of Volcanology and Geothermal Research* **55**, 18–48.

Stubley, M. (2000). Bedrock geology of the Snap Lake area, Camsell Lake Property: a report to accompany a 1:10,000 scale geological map. Unpublished report, prepared for Winspear Resources Ltd, Vancouver.

Tuttle, O. F. & Bowen, N. L. (1958). Origin of granite in the light of experimental studies in the system $NaAlSi_3O_8$–$KAlSi_3O_8$–SiO_2–H_2O. *Geological Society of America Memoirs* **74**, 1–145.

Wares, R. P. & Martin, R. F. (1980). Rodingitization of granite and serpentinite in the Jeffrey Mine, Asbestos, Quebec. *The Canadian Mineralogist* **18**, 231–240.

Wones, D. R. & Eugster, H. P. (1965). Stability of biotite: experiment, theory and application. *The American Mineralogist* **50**, 1228–1272.